Solid Freeform Fabrication 2022: Proceedings of the 33rd Annual International Solid Freeform Fabrication Symposium – An Additive Manufacturing Conference
Reviewed Paper

Effects of Process Interruption During Laser Powder Bed Fusion on Microstructural and Mechanical Properties of Fabricated Parts

MohammadBagher Mahtabi[1], Aref Yadollahi[1*], Ryan Stokes[2], Joseph Young[3], Haley Doude[3], Matthew W. Priddy[2], Linkan Bian[3,4]

[1]William B. Burnsed, Jr. Department of Mechanical, Aerospace, and Biomedical Engineering, University of South Alabama, Mobile, AL 36688, USA

[2]Department of Mechanical Engineering, Mississippi State University, Mississippi, 39762, USA

[3]Center for Advanced Vehicular Systems (CAVS), Starkville, Mississippi, MS, 39759, USA

[4]Department of Industrial and Systems Engineering, Mississippi State University, Mississippi, 39762, USA

*Corresponding Author, Phone: (251) 460-7706, e-mail: ayadollahi@southalabama.edu

Abstract

Despite appropriate planning, various incidents can stop the additive manufacturing (AM) process of metals and cause build interruption, such as power outage, lack of powder feedstock, and/or shielding gas to mention a few. Due to the layer-by-layer nature of fabrication, an interruption to the AM process can be resumed from the location where the stoppage occurred. However, build interruption may adversely affect the structural integrity of the fabricated parts, by causing localized failure near the interruption location. This study aims to investigate the influence of build interruption during the laser powder bed fusion (LPBF) process on the microstructural and mechanical properties of Ti-6Al-4V and Al-Si-10Mg specimens. For the Ti-6Al-4V specimens, results indicate that tensile failures near the interruption location are most likely to happen for non-heat-treated specimens in the as-built surface condition. Whereas for the Al-Si-10Mg specimens, the failure location is more influenced by the prolonged stoppage and air exposure.

Keywords: Build interruption; Additive manufacturing (AM); Failure location; Al-Si-10Mg; Ti-6Al-4V

1. Introduction

In recent years, additive manufacturing (AM) has opened new avenues for fabricating metallic parts with complex geometries [1]. Laser powder bed fusion (LPBF) is one of the most broadly applied techniques in metal AM that receives more and more attention in the industry and academia [2]. Due to the relatively low build rate of the LPBF process, fabrication of large components will be time-consuming, thus any interruption to the process during the build could result in loss of time and money. Despite appropriate planning and procedures, various incidents may stop the LPBF process, such as lack of powder quantities, power outage, faulty build data, or various probable incidents. Due to the layer-by-layer nature of the fabrication, an interruption to the LPBF process can be resumed from the location where the stoppage occurred. Although a continuation of the process at the stoppage location will be economic and time-saving, build interruption may adversely affect the structural integrity of the fabricated parts by causing localized failure near the interruption plane. This is due to the fact that any stop/start during the fabrication affects the thermal history, leading to changes in the microstructures and residual stresses, and consequently, the mechanical properties of the part.

Despite significant research efforts focused on the effect of process parameters and build conditions [3–8] on the microstructural features and mechanical properties of LPBF parts, to date there have only been a few studies characterizing LPBF process/build interruption effects on the properties of fabricated parts [9–15]. Terrazas-Najara et al. studied the effect of process interruption on the microstructure and tensile properties of LPBF Inconel 625, Inconel 718, and Al-Si-10Mg alloys. They applied two different protocols for a time span of one hour by keeping the coupons either in an air exposure condition or in a condition where the chamber remained closed. Their results showed that neither microstructures nor tensile properties appeared to be sensitive to process interruption [9]. Binder et al. studied the effect of a 40-minute process interruption along with air exposure on LPBF Al-Si-10Mg. They showed that almost all the interrupted samples, fabricated in a vertical direction, were broken at the interruption plane under monotonic tensile testing. They have also reported that the process interruption, accompanied by remelting, affected the tensile properties of the samples [10]. Stoll et al. showed that a 60-minute process interruption for 316L stainless steel (SS) samples caused a reduction in tensile strength. In their work, the chamber was opened, and the powder bed was allowed to cool down to room temperature. They also reported that the location of the tensile failure is not necessarily depended on the process interruption [12], opposite to what has been reported for the LPBF Al-Si-10Mg [10,11]. Hammond et al. reported that the tensile strength and microhardness values of interrupted Al-Si-10Mg samples were 10% lower compared to the samples fabricated without interruption. In their study, the majority of the interrupted samples failed near the interruption plane under the monotonic tensile testing [11]. Richter et al. studied the microstructures, tensile, and fatigue properties of LPBF AlSi12 influenced by the process interruption. Their microstructural observations revealed a distinct distortion in grain morphology at the plane of interruption; however, tensile strength of interrupted and non-interrupted samples was almost similar, and the location of failure in tensile and fatigue tests did not coincide with the interruption plane [13].

The literature on build interruption during the LPBF process contains studies where the findings of one study either contradict or cannot be directly compared with those of another, mainly due to the differences in the material system and the conditions of interruption (i.e., duration of the

interruption, air exposure, etc.). Thus, more methodical research is needed to understand the effect of build interruption on the microstructural properties and mechanical performance of different alloys fabricated via LPBF process. The duration for which the LPBF machine is shut-down due to an interruption is a function of the type of interruption, which can significantly affect the thermal history, and consequently, the microstructural features (e.g., grain size) and residual stresses in the vicinity of the interruption plane. In addition, the purge gas flow typically stops after a machine stoppage. Lack of shielding gas could allow oxygen to reach the melt tracks, which could be detrimental to the quality of the part. Particularly, for the LPBF Al-Si-10Mg, the formation of oxide films during processing can be a cause of porosity. Furthermore, improper powder application upon resuming the build can lead to inadequate melting, increasing the chance of lack-of-fusion (LOF) defects. This study aims to investigate the effects of various conditions of build interruption (i.e., duration of the interruption and air exposure), surface finish, and heat treatment on the microstructural and mechanical properties of LPBF Al-Si-10Mg and Ti-6Al-4V alloys.

2. Experimental Procedure

The Al-Si-10Mg and Ti-6Al-4V samples for this study were fabricated via an LPBF system (Renishaw AM 400) in a vertical direction. The chemical composition of the utilized powders, provided by the manufacturer (LPW, US), is given in Table 1. Optimized process parameters, recommended by Renishaw, were used for the fabrication of the Al-Si-10Mg and Ti-6Al-4V samples in both interrupted and non-interrupted (i.e., control) conditions. The utilized process parameters are reported in Table 2. Samples were fabricated in dogbone and cylindrical shape to study the effect of surface conditions on the monotonic tensile behavior, as shown in Figures 1(a) and (b), respectively. After the fabrication, cylindrical samples were machined into the dogbone shape, with the same geometry as those directly fabricated in dogbone shape in accordance with ASTM E8/E8M [16]. Dimensions and configurations of the sample, as well as the location of interruption, are illustrated in Figure 1.

Table 1. Chemical composition of the Al-Si-10Mg and Ti-6Al-4V powders.

Material	Chemical composition (wt. %)
Al-Si-10Mg	Si 11.0, Mg 0.35, Fe 0.11, O 0.04, Al balance
Ti-6Al-4V	Al 6.40, V 4.10, C 0.01, H 0.0029, O 0.11, N 0.02, Fe 0.21, Ti balance

Table 2. Process parameters utilized for fabrication of Al-Si-10Mg and Ti-6Al-4V samples.

Material	Laser power (W)	Scan speed (mm/s)	Layer thickness (µm)	Preheated platform (Celsius)
Al-Si-10Mg	275	2000	30	170
Ti-6Al-4V	200	1100	30	170

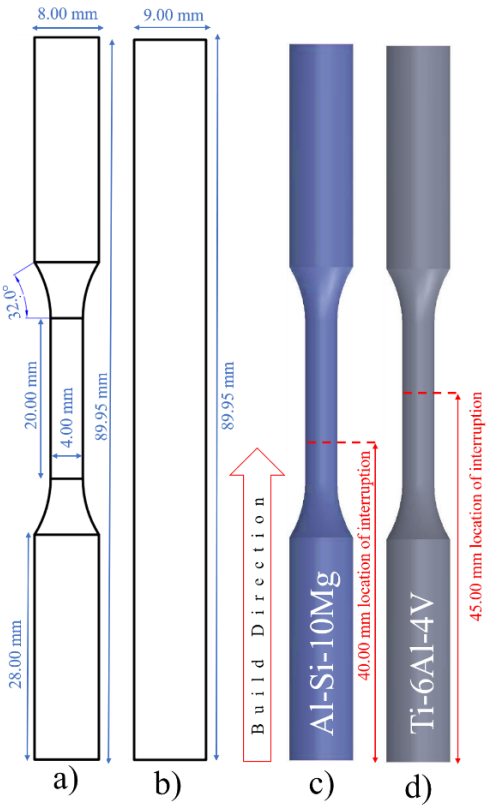

Figure 1. Schematic showing the geometry and configuration of (a) dogbone, (b) cylindrical samples, and location of interruption for (c) Al-Si-10Mg and (d) Ti-6Al-4V tensile specimens.

For the Al-Si-10Mg samples, seven builds, including control and six interrupted builds were investigated. Three interruption protocols were implemented to simulate real-life scenarios that might occur during LPBF processing: (i) pausing the machine to refill unplanned powder runout (15 MIN), (ii) an unexpected power outage requiring significant intervention (12 HR), and (iii) a machine that faults for a prolonged period during unattended hours (24 HR) and each protocol was repeated with and without an air exposure during the interruption period [15]. For the Ti-6Al-4V samples, the process interruption lasted for 24 hours, and the machine was paused halfway through the height of the specimens with no air exposure. Tables 3 and 4 present an overview of the interruption procedures for Al-Si-10Mg and Ti-6Al-4V samples.

To simulate the interruption, each build was paused at the same layer number of the level of interruption (i.e., at the height of 40mm for Al-Si-10Mg and 45mm for Ti-6Al-4V samples) to place the interruption level within the gage section. Machine operation was resumed after finishing the interruption protocols (time period and air exposure) for Al-Si-10Mg and Ti-6Al-4V samples, except for 12 HR Al-Si-10Mg samples. In 12 HR samples, since the heated build platform (BP) was turned off during the interruption. Because of the cooling and contraction within the elevator and samples, it was indispensable to adjust the elevator's height to ensure powder spreading was occurring properly. Several test wiper spreads were done to ensure a thin layer height appropriate; spread of powder was evident on each specimen. After this was deemed sufficient, the machine was restarted [14].

Table 3. Interruption condition for Al-Si-10Mg samples.

Experiment group		Interruption time	Air exposure	Heated BP	Surface finish	HT	Group ID
Al-Si-10Mg	1	Control	No	On	As-built	No	C-A0-HBP
	2	12 HR	No	Off	As-built	No	12-A0
	3	24 HR	No	On	As-built	No	24-A0-HBP
	4	15 MIN	Yes	On	As-built	No	15-A1-HBP
	5	15 MIN	No	On	As-built	No	15-A0-HBP
	6	12 HR	Yes	Off	As-built	No	12-A1
	7	24 HR	Yes	On	As-built	No	24-A1-HBP

Table 4. Interruption condition for Ti-6Al-4V samples.

Experiment group		Interruption time	Air exposure	Heated BP	Surface finish	HT	Group ID
Ti-6Al-4V	1	Control	No	On	As-built	No	ABC
	2	Control	No	On	Machined	No	MC
	3	Control	No	On	As-built	Yes	ABC_HT
	4	Control	No	On	Machined	Yes	MC_HT
	5	24 HR	No	On	As-built	No	ABI
	6	24 HR	No	On	Machined	No	MI
	7	24 HR	No	On	As-built	Yes	ABI_HT
	8	24 HR	No	On	Machined	Yes	MI_HT

In order to study the interaction of heat treatment (HT) with the process interruption effects on the microstructure, residual stress, and consequently the mechanical performance, the Ti-6Al-4V samples were annealed at 760 °C for 1 hour in an inert Argon atmosphere, followed by air cooling. This procedure allows for stress relief and decomposition of the martensitic phase [17,18]. No heat treatment was done for the Al-Si-10Mg specimens.

In order to quantitatively assess the formation of any possible process-induced defects near the interruption location, the gage section of the tensile specimens was scanned using an X-ray computed tomography (XCT) system. Microhardness distribution was measured along the build direction (within the gage section) via a Vickers microhardness tester (Leco Vicker LM-300AT) under a 500-g load for a dwell time of 10 s using a diamond indenter. Monotonic tensile tests were conducted on three specimens in each group under strain-controlled conditions at a 0.001/s nominal strain rate for both Al-Si-10Mg and Ti-6Al-4V. Finally, microstructures and fracture surfaces were observed using scanning electron microscopy (SEM).

3. Results and Discussion

3.1. Microstructural characterization

The process interruption may increase the probability of occurrence of process-induced defects, i.e., gas pores and LOFs, as a result of change in the melt pool dynamics and unsustainable bonding between layers. Analysis of our XCT results for Al-Si-10Mg samples showed no meaningful correlation between the formation of defects within the interruption zone and the interruption conditions (i.e., air exposure and interruption time). However, XCT results for Ti-6Al-4V samples revealed a significant increase in the total volume of defects near the interruption zone.

In order to investigate the changes in microstructural features near the interruption zone, samples were cut ~5 mm above and below the interruption interface. For Al-Si-10Mg, SEM image shown in Figure 2 displays the microstructure of the interrupted specimen near the interruption location in 24 HR/air exposure condition. A visible line of discoloration can be seen near the interruption plane, which can be attributed to the changes in thermal history due to the process interruption. This feature was observed for all 24 HR specimens. For the Ti-6Al-4V samples, microstructural features in the vicinity of the interruption zone showed no qualitative difference compared to the control counterparts.

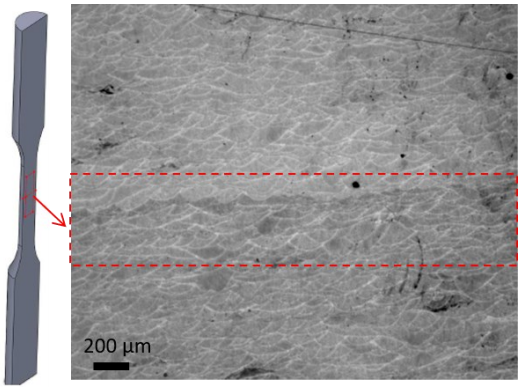

Figure 2. SEM image of microstructures for Al-Si-10Mg interrupted sample in 24 HR/air exposure condition.

Figure 3 shows the SEM micrographs for Ti-6Al-4V samples fabricated in the dogbone and cylinder shapes, before (NHT) and after heat treatment (HT). As can be seen in Figures 3(a) and (b), the characteristic of melt-pool banding patterns was visible only for the non-heat-treated samples. The microstructure of dogbone and cylindrical samples after heat treatment are shown in Figures 3(c) and (d), respectively. The utilized annealing resulted in homogenization of microstructure and removed the interfacial regions.

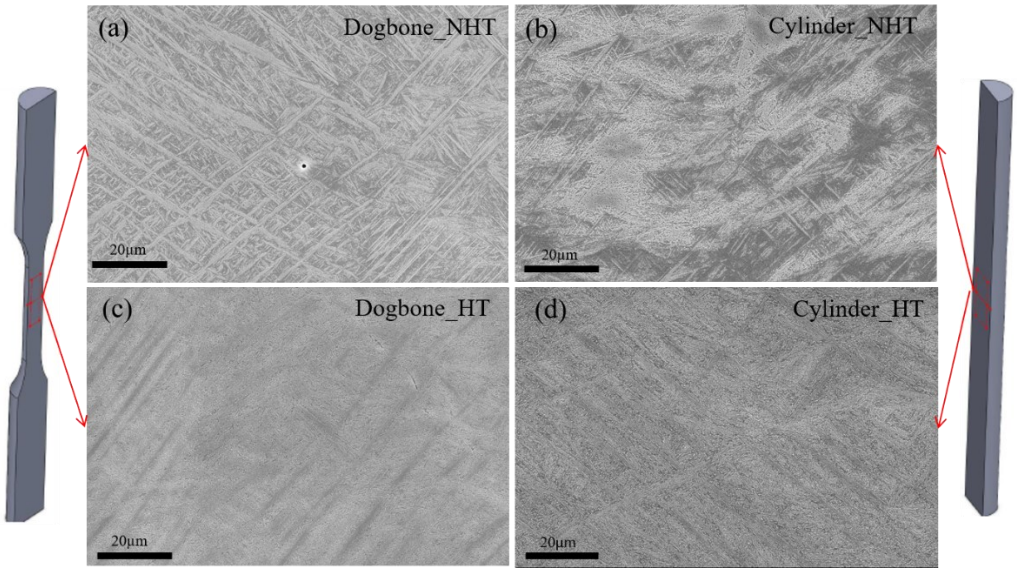

Figure 3. SEM images of microstructures for Ti-6Al-4V interrupted specimens in (a) dogbone_NHT, (b) cylinder_NHT, (c) dogbone_HT, and (d) cylinder_HT conditions.

To explore any unexpected changes in the distribution of microhardness values near the interruption location, several microhardness measurements were taken along the build direction, passing across the interruption level. Results for both Al-Si-10Mg and Ti-6Al-4V samples showed no distinctive changes in the distribution of hardness values near the location of interruption. The average Vickers microhardness values for the Al-Si-10Mg and Ti-6Al-4V samples were 135 HV and 425 HV, respectively.

3.2. Monotonic tensile test

Monotonic tensile tests were performed to investigate the potential relationship between the process interruption and tensile properties, including yield stress, ultimate tensile strength, and elongation to failure, as well as the location of failure. The results of the tensile tests for Al-Si-Mg and Ti-6Al-4V specimens are shown in Figures 4 and 5, respectively.

For the Al-Si-10Mg specimens, results revealed that yield stress, ultimate tensile strength, and elongation to failure for all the specimens were almost similar, regardless of the interruption time and air exposure, as can be seen in Figures 4(a) and (b). Values for ultimate tensile strength as well as the location of failure for Al-Si-10Mg samples agree with the results reported by Binder et al. [10].

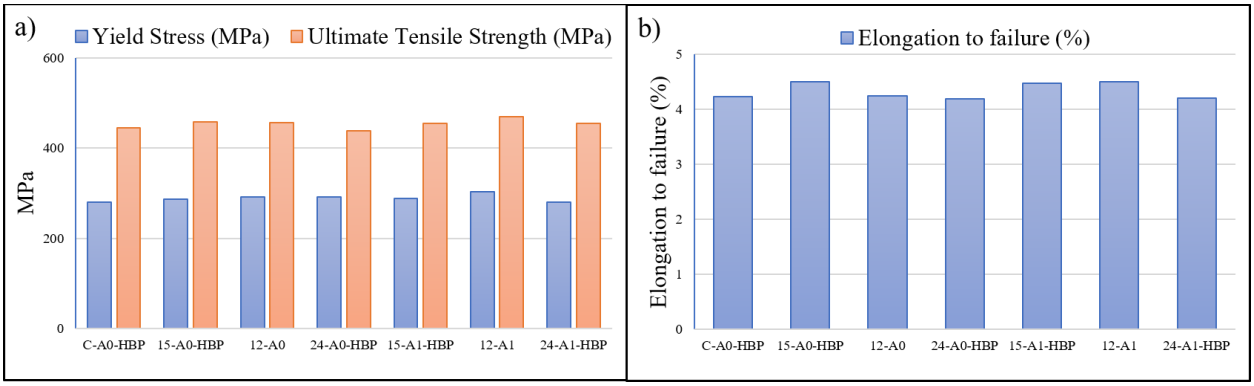

Figure 4. (a) Yield stress, ultimate tensile strength, and (b) elongation to failure values obtained for Al-Si-10Mg specimens.

For the Ti-6Al-4V specimens, as seen in Figure 5, the utilized annealing caused an increase in ductility and a decrease in the ultimate tensile strength, where all of the non-heat-treated specimens had higher elongation to failure and lower ultimate tensile strength compared to their heat-treated counterparts. In addition, as can be seen in Figure 5(a), the machined specimens appeared to have higher ultimate tensile strength than the as-built samples, regardless of being affected by the process interruption. As shown in Figure 5(b), the elongation to failure for all interrupted specimens was lower than their control counterparts. The least elongation to failure belonged to the interrupted specimens with as-built surface condition. The fracture location of one the as-built specimen was coincident with the interrupted plane, as shown in Figure 7.

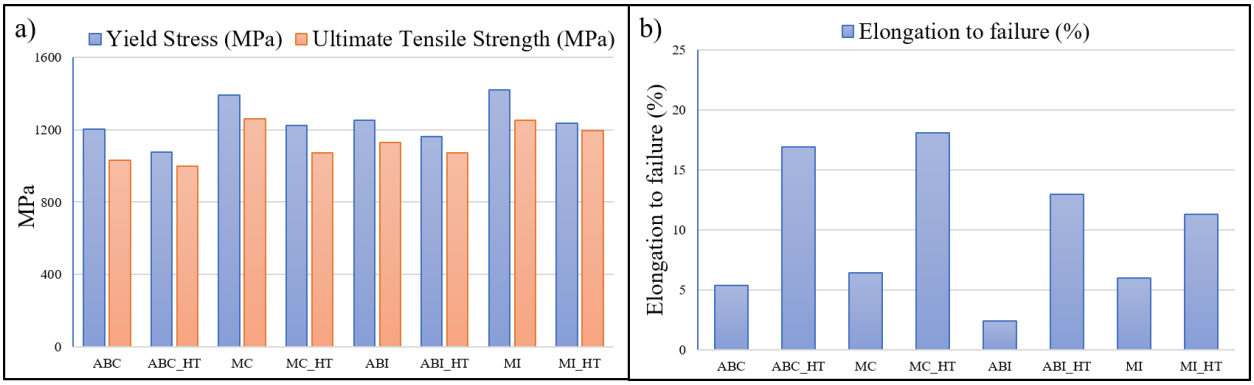

Figure 5. (a) Yield stress, ultimate tensile strength, and (b) elongation to failure values obtained for Ti-6Al-4V specimens.

3.3. Fractography

SEM micrograph of tensile fracture surfaces of Al-Si-10Mg and Ti-6Al-4V specimens are presented in Figures 6 and 7. For Al-Si-10Mg, almost half of the interrupted specimens, particularly 24 HR air exposure ones, failed near the interruption location. Tensile fracture surfaces and the location of failure for the 24 HR air exposure group are shown in Figure 6. It can be seen in Figure 6(a) that the location of failure for two out of three specimens in this group is coincident with the interruption level. A large number of gas-pores (shown by arrow) were observed on the fracture surface of the interrupted Al-Si-10Mg specimens that failed at the interruption level, as can be seen in Figure 6(b). However, it cannot be concluded that these gas pores are formed due to the process interruption since other interrupted specimens that did not fail at the interruption plane have the same amount of gas pores on their fracture surface, as can be seen in Figure 6(c).

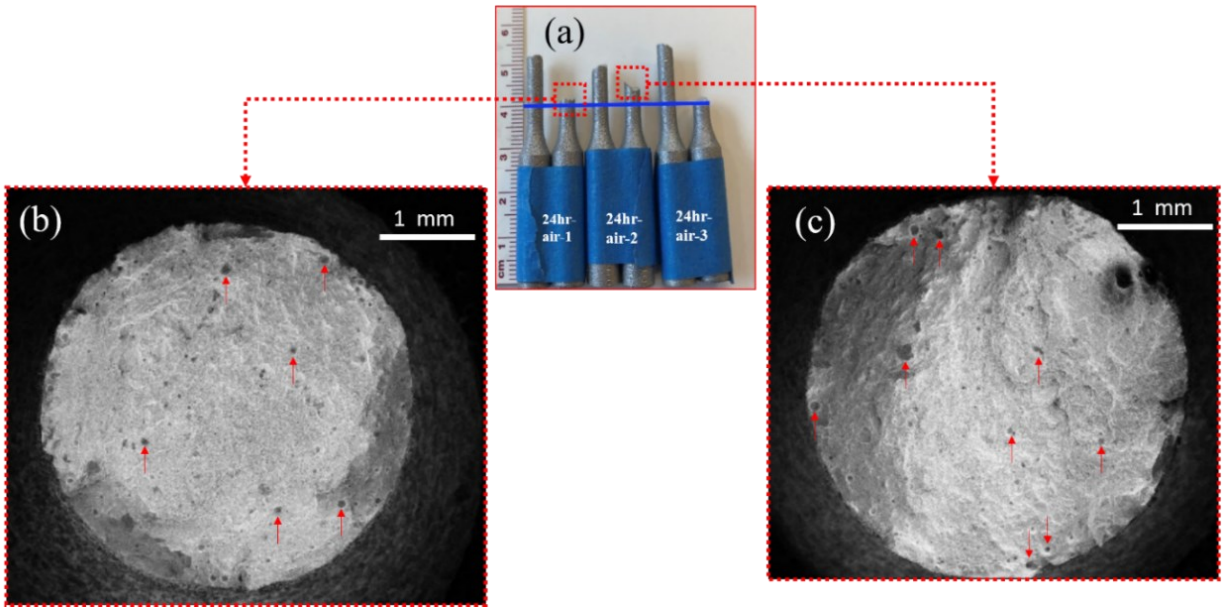

Figure 6. (a) Location of failure for the Al-Si-10Mg specimens in the 24 HR with air exposure group, along with the SEM images of tensile fracture surface for the specimens failed (b) near and (c) above the interruption plane.

For Ti-6Al-4V specimens, the location of failure for the non-heat-treated specimens in the as-built surface condition was coincident with the location of interruption. This indicates that post-fabrication heat treatment and surface finishing can minimize any potential influence of build interruption on the failure location. The fracture surface of this specimen is presented in Figure 7, where LOF defects and gas pores can be observed on the fracture surface.

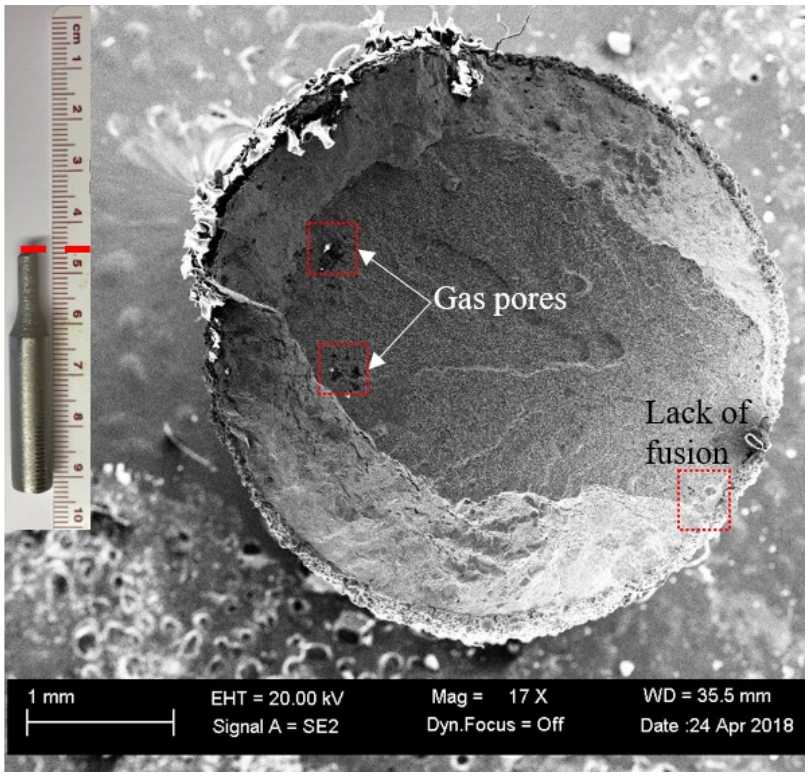

Figure 7. Tensile fracture surface of non-heat-treated interrupted Ti-6Al-4V specimen in the as-built condition.

4. Summary

In this study, the effects of various conditions of build interruption (i.e., duration of the interruption and air exposure) as well as post-fabrication heat treatment and surface finishing on the microstructural and mechanical properties of LPBF Al-Si-10Mg and Ti-6Al-4V alloys were investigated, and the results were compared with those from a continuous fabrication route. For the Al-Si-10Mg specimens, monotonic tensile tests showed half of the interrupted specimens failed near the interruption location, particularly the specimens with prolonged interruption time and air exposure (24 HR). Tensile and microhardness tests did not show any distinctive changes in the tensile strength and microhardness values as compared to their control counterparts (i.e., non-interrupted). For the Ti-6Al-4V specimens, the tensile location of failure for one of the non-heat-treated specimens in the as-built surface condition (i.e., dogbone specimens) was coincident with the interruption location. In addition, all interrupted Ti-6Al-4V specimens showed a lower elongation to failure as compared to the control specimens. Similar to the Al-Si-10Mg samples, Ti-6Al-4V samples showed no distinctive changes in the distribution of hardness values near the interruption locations. More studies are still required to evaluate the effect of build interruption on other mechanical properties, such as fatigue and creep.

5. References

[1] Yadollahi A, Shamsaei N. Additive manufacturing of fatigue resistant materials: Challenges and opportunities. Int J Fatigue 2017;98:14–31.

[2] ASTM. ASTM Standard F2792-12a: Standard Terminology for Additive Manufacturing Technologies 2015.

[3] Yadollahi A, Shamsaei N, Thompson SM, Elwany A, Bian L. Effects of building orientation and heat treatment on fatigue behavior of selective laser melted 17-4 PH stainless steel. Int J Fatigue 2017;94:218–35.

[4] Criales LE, Arısoy YM, Lane B, Moylan S, Donmez A, Özel T. Laser powder bed fusion of nickel alloy 625: Experimental investigations of effects of process parameters on melt pool size and shape with spatter analysis. Int J Mach Tools Manuf 2017;121:22–36.

[5] Shi Y, Yang K, Kairy SK, Palm F, Wu X, Rometsch PA. Effect of platform temperature on the porosity, microstructure and mechanical properties of an Al–Mg–Sc–Zr alloy fabricated by selective laser melting. Materials Science and Engineering: A 2018;732:41–52.

[6] Malỳ M, Höller C, Skalon M, Meier B, Koutnỳ D, Pichler R, et al. Effect of Process Parameters and High-Temperature Preheating on Residual Stress and Relative Density of Ti6Al4V Processed by Selective Laser Melting. Materials 2019, Vol 12, Page 930 2019;12:930.

[7] Yadollahi A, Mahtabi MJ, Khalili A, Doude HR, Newman JC. Fatigue life prediction of additively manufactured material: Effects of surface roughness, defect size, and shape. Fatigue Fract Eng Mater Struct 2018;41:1602–14.

[8] Marola S, Manfredi D, Fiore G, Poletti MG, Lombardi M, Fino P, et al. A comparison of Selective Laser Melting with bulk rapid solidification of AlSi10Mg alloy. J Alloys Compd 2018;742:271–9.

[9] Terrazas-Najera CA, Mayoral FL, Garcia OF, Hossain MS, Espalin D, Fernandez A, et al. Effects of process interruptions on microstructure and mechanical properties of three face centered cubic alloys processed by laser powder bed fusion. J Manuf Process 2021;66:397–406.

[10] Binder M, Leong C, Anstaett C, Schlick G, Seidel C, Reinhart G. Effects of process interruptions on the microstructure and tensile properties of AlSi10Mg parts manufactured by Laser-Based Powder Bed Fusion. Procedia CIRP 2020;94:182–7.

[11] Hammond V, Schuch M, Bleckmann M. The influence of a process interruption on tensile properties of AlSi10Mg samples produced by selective laser melting. Rapid Prototyp J 2019;25:1442–52.

[12] Stoll P, Spierings A, Wegener K. Impact of a process interruption on tensile properties of SS 316L parts and hybrid parts produced with selective laser melting. International Journal of Advanced Manufacturing Technology 2019;103:367–76.

[13] Richter J, Sajadifar S v., Niendorf T. On the influence of process interruptions during additive manufacturing on the fatigue resistance of AlSi12. Addit Manuf 2021;47:102346.

[14] Stokes RM, Yadollahi A, Priddy MW, Bian L, Hammond VH, Doude HR. Effects of Build Interruption and Restart Procedure on Microstructure and Mechanical Properties of Laser Powder Bed Fusion Al-Si-10Mg. Journal of Materials Engineering and Performance 2022 2022:1–13.

[15] Ryan Mitchell Stokes. Characterizing the effects of build interruptions on the microstructure and mechanical properties of powder bed fusion processed Al-Si-10Mg. Mississippi State University, 2019.

[16] ASTM E8/E8M : Standard Test Methods for Tension Testing of Metallic Materials. 2022.
[17] Zhai Y, Galarraga H, Lados DA. Microstructure, static properties, and fatigue crack growth mechanisms in Ti-6Al-4V fabricated by additive manufacturing: LENS and EBM. Eng Fail Anal 2016;69:3–14.
[18] Fousová M, Dvorský D, Michalcová A, Vojtěch D. Changes in the microstructure and mechanical properties of additively manufactured AlSi10Mg alloy after exposure to elevated temperatures. Mater Charact 2018;137:119–26.